

Inertial Screening in Sedimentation

P.N. Segrè

Department of Physics, Emory University, Atlanta, GA 30322

Abstract

We use particle image velocimetry to measure the sedimentation dynamics of a semi-dilute suspension of non-Brownian spheres at Reynolds numbers, $0.001 \leq Re \leq 2.3$, extending from the Stokes to the moderately inertial regime. We find that the onset of inertial corrections to Stokes sedimentation occurs when the inertial screening length $l = a/Re$ becomes similar to the Stokes sedimentation length ξ_0 , at $Re_c = a/\xi_0 \approx 0.05$. For $Re > Re_c$, inertial screening significantly reduces both the magnitude and spatial extent of the particle velocity fluctuations. A modified Hinch force balance model connects the fluctuation magnitudes σ_V/V to the correlation sizes ξ .

The sedimentation dynamics of non-Brownian spheres is a fundamental problem in physics [1] and has been the subject of intense activity in recent years (for a review see [2]). Much of the focus has been on particles slowly settling in viscous liquids, conditions that correspond to very low Reynolds numbers, $Re \ll 1$, called the Stokes regime. The Reynolds number is the ratio of inertial to viscous forces in fluids, and is defined as $Re \equiv 2Va/\nu$ (V is the particle velocity, a the radius, and ν the fluid kinematic viscosity). In the Stokes regime, where inertial forces are insignificant, concentrations of spheres display Re -independent large amplitude velocity fluctuations σ_V/V during settling [3, 4, 5, 6, 7]. Significantly, experiments [5, 6, 7, 8], simulations [9], and theory [10] have shown that the fluctuations display a characteristic spatial size ξ , despite the fact that the hydrodynamic interactions emanating from a single *isolated* sphere are of infinite range ($\propto 1/r$) [11]. The Stokes screening length ξ represents regions of concentration fluctuations, σ_ϕ , that drive velocity fluctuations σ_V and particle diffusion $D \sim \sigma_V \xi$. While an explanation of the origin of screening in Stokes sedimentation remains controversial, its existence and central importance for a description of sedimentation is not.

The sedimentation dynamics at higher speed flows where inertial forces become significant, $Re \sim 1$, have received much less attention despite its fundamental importance and widespread relevance to numerous chemical industries [12]. In contrast to the Stokes regime, for an *isolated* sphere falling at moderate Re , there is a distance beyond which the $1/r$ Stokes like hydrodynamics are screened [11]. The inertial screening length, $l \sim a/Re$, becomes shorter as the Reynolds number is increased. For concentrations of settling spheres, the Reynolds number dependence of the hydrodynamic interactions brought about by inertia is predicted to result in Reynolds number dependent sedimentation dynamics as well [13]. Experiments designed to investigate these changes, however, are greatly lacking. We are aware of only a single experiment, by Cowan et al. [14] using novel ultrasonic techniques, that has examined the fluctuation dynamics of spheres at moderate $Re \lesssim 1$. Surprisingly, they concluded that the velocity fluctuations were independent of Reynolds number for $Re \lesssim 1$. In the absence of experiments describing the sedimentation dynamics beyond the Stokes regime, our understanding of the basic physics, and our ability to develop and test model theories, remains very limited.

In this letter, we describe experiments that demonstrate how moderate amounts of fluid inertia can significantly affect the settling dynamics of spheres. The onset of inertial correc-

tions to Stokes sedimentation occurs when the inertial screening length $l = a/Re$ becomes as small as the Stokes sedimentation length ξ_0 , at $Re_c = a/\xi_0$. For $Re > Re_c$, inertial screening significantly reduces both the magnitude and spatial extent of the particle velocity fluctuations. A modified Hinch force balance model, with Reynolds number dependent drag coefficients, connects the fluctuation magnitudes σ_V/V to the correlation sizes ξ over the entire range studied, $0.001 \leq Re \leq 2.3$.

The particles used in our experiments were monodisperse glass beads of radius $a = 137 \pm 9 \mu\text{m}$. They were dispersed in various mixtures of glycerol and water, enabling us to examine the very low to moderate Reynolds number regimes, $0.001 \leq Re \leq 2.3$. In all cases the volume fraction is $\phi = 0.06$. The sample cell was a rectangular glass tube of dimension $8 \times 80 \times 305 \text{ mm}$, and the temperature was at the ambient value $T = 23 \pm 1^\circ\text{C}$. Particle velocities were measured using a particle image velocimetry (PIV) [15] apparatus consisting of some specialized image processing software and hardware purchased from Dantec Instruments. A large cross section of the cell was imaged ($3 \times 3 \text{ cm}$), so that several thousand particles could be simultaneously studied. Initially, random dispersions were prepared by vigorous shaking of the cells. The location of the imaging window was far from both the sedimentation front and the sediment growth. Each velocity fields is a map of 41×42 vectors, and each velocity vector is the local average of two to four spheres.

We begin by examining typical particle velocity fields during sedimentation. Figures 1(a-c) show results for particle velocities \mathbf{V}_i from three samples spanning the very low, $Re = 0.001 \ll 1$, to moderate, $Re = 2.3$, Reynolds number regimes. In the Stokes flow regime, Fig. 1(a), the patterns look similar to those reported in the literature [5, 7], with large magnitude fluctuations occurring in extended *swirling* regions. In the presence of some inertia, $Re = 0.2$ in Fig. 1(b), the pattern appears slightly more uniform, indicating a slight reduction in the fluctuations relative to that seen at $Re = 0.001$. At the highest flow speed, $Re = 2.3$ in Fig. 1(c), there is a dramatic change in the dynamics. The fluctuations are largely absent, the particles appear to be nearly falling with the same speed. We interpret these changes as evidence of an inertial screening of the velocity fluctuations.

To examine the fluctuations in more detail, Figs. 1(d-f) shows the same set of maps with the mean velocities subtracted off, $\delta\mathbf{V}_i \equiv \mathbf{V}_i - \langle\mathbf{V}_i\rangle$. All of the patterns in fact show qualitatively similar swirling regions. The sizes of the regions appear to decrease with Re . The dramatic decrease in fluctuations seen in Fig. 1(c) is reflected in the greatly magnified

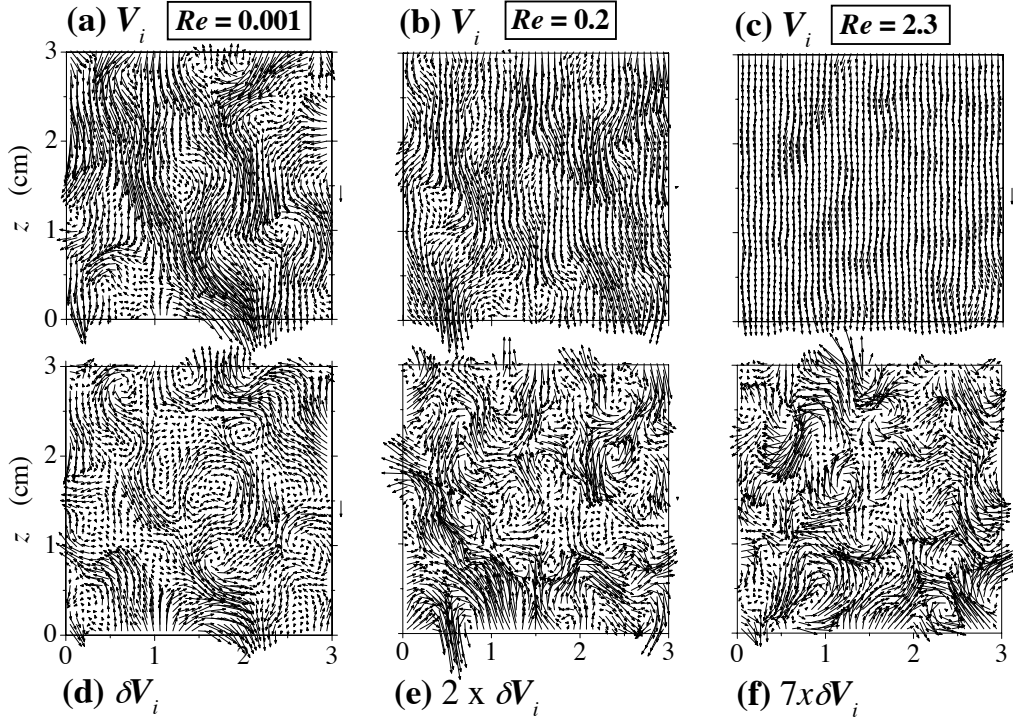


FIG. 1: PIV results for three suspensions of sedimenting spheres at $\phi = 0.06$ and Reynolds numbers (a,d) $Re = 0.001$, (b,e) $Re = 0.2$, and (c,f) $Re = 2.3$. (a-c) Velocities \mathbf{V}_i . (d-f) Velocity fluctuations calculated from (a-c) using $\delta\mathbf{V}_i = \mathbf{V}_i - \langle\mathbf{V}_i\rangle$. (Note the magnified scales in (e,f)). The single vector to the right of each map represents the mean velocity $\langle\mathbf{V}_i\rangle$.

scale ($7 \times \delta\mathbf{V}_i$) of Fig. 1(f) relative to Fig. 1(d).

By collecting large numbers of velocity maps over the majority of each falling column, we can access ensemble averaged information. We first examine the spatial correlations of the velocity fluctuations. The normalized autocorrelation function of the z component (\parallel to gravity) of the velocity fluctuations is defined as $C_z(\mathbf{r}) \equiv \langle\delta V_z(0)\delta V_z(\mathbf{r})\rangle/\langle\delta V_z(0)^2\rangle$, where $\langle\dots\rangle$ represents an ensemble average of several hundred vector maps. The distance vector \mathbf{r} is either in the direction parallel to gravity, $C_z(z)$, or perpendicular to it, $C_z(x)$.

To search for evidence of inertial screening in the spatial velocity correlations, Fig. 2 compares the correlation functions between a sample in the Stokes regime, $Re = 0.001$, and one with significant inertia, $Re = 2.3$. In all cases the functions decay to zero at large distances, indicative of finite range correlations. The decay lengths, however, are much reduced in the inertial sample. The form of the perpendicular correlation function is also affected, the long-range negative correlation dip in $C_z(x)$ is completely absent in the inertial

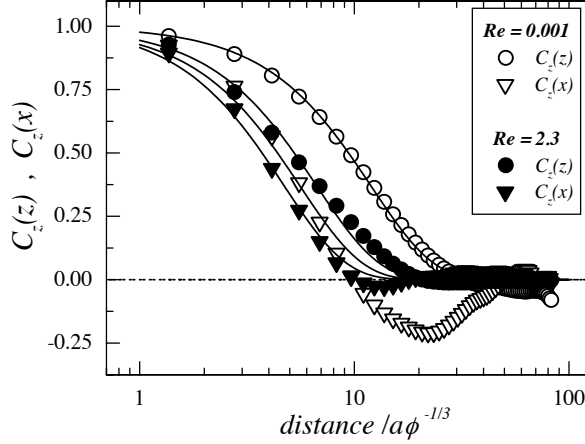


FIG. 2: Spatial correlation functions of the z component of the velocity fluctuations as a function of distance \parallel , $C_z(z)$, and \perp , $C_z(x)$, to the z -axis for $Re = 0.001$ and $Re = 2.3$.

case.

To quantify the range of the velocity correlation functions, we fit to the empirical forms $C_z(z) = \exp[-(z/\xi)^{1.5}]$ and $C_z(x) = \exp[-(x/\xi_\perp)^{1.5}]$, as shown in Fig. 2. Results are given in Fig. 3(a) for ξ and ξ_\perp from all of our samples ranging from $0.001 \leq Re \leq 2.3$. The longitudinal length ξ , the longer of the two, shows the most change with Re . For $Re \lesssim 0.05$, ξ is independent of Re as expected in the Stokes regime, and the values are all in good agreement with the scaling relation $\xi_0 \approx 11a\phi^{-1/3}$ previously found in very low Reynolds number sedimentation [5]. For $Re \gtrsim 0.05$, the behavior begins to change, and ξ follows a roughly logarithmic decay with Re . The decrease of ξ with Re demonstrates that inertial screening occurs at shorter distances for higher Reynolds numbers. In agreement with this, the short range transverse correlations don't show any inertial influence until much higher Reynolds numbers, $Re = 2.3$. For analysis purposes below, we note that ξ can be well fit by

$$\xi \simeq \xi_0 / (1 + 5.5Re)^{1/4}. \quad (1)$$

The velocity maps in Fig. 1 also show dramatic changes to the *magnitudes* of the velocity fluctuations as Re is increased. To quantify this we consider the ensemble averaged *rms* velocity fluctuations, $\sigma_v \equiv \sqrt{\langle [V_{i,z} - V]^2 \rangle}$, with results for the normalized values σ_v/V shown in Fig. 3(b). σ_v/V is independent of Re for $Re \lesssim 0.05$, as expected in the Stokes regime, and the value $\sigma_v/V \approx 0.75$ is in good agreement with results found in Stokes flow sedimentation [4, 5, 6]. In a similar way to that seen for ξ vs. Re , the onset of inertial

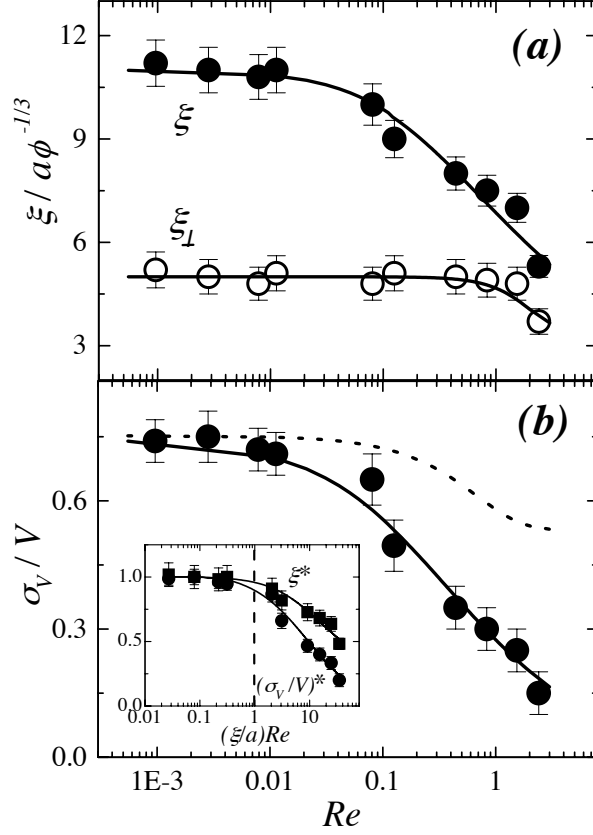


FIG. 3: Inertial screening of velocity fluctuations. (a) Spatial correlation lengths ξ and ξ_{\perp} as a function of Reynolds number Re . The line through ξ is the empirical fit Eq. (1). The line through ξ_{\perp} is a guide to the eye. (b) Normalized velocity fluctuations σ_V/V vs. Re . The solid line is the Hinch model Eq. (2). The dashed line is Eq. (2) with $Re = 0$. Inset: ξ and (σ_V/V) , normalized by their Stokes values, vs. $(\xi/a)Re$.

influence occurs at $Re \approx 0.05$, and at higher speeds the fluctuations sharply decline with Re . At our highest speed, $Re = 2.3$, σ_v/V is reduced by $\approx 80\%$.

We now address whether the dependencies found for the correlation lengths and the fluctuation magnitudes can be interrelated by a simple extension of the Hinch model [1, 16] that was originally developed for the Stokes regime [1, 5, 6]. Within this model, velocity fluctuations arise from particle density fluctuations in regions whose spatial extent is the correlation length ξ . For a *random* particle configuration, the average number of particles in a region of size ξ is $N_{\xi} = \xi^3 \phi / v_p$, where $v_p = 4\pi a^3/3$. The fluctuations in number are $\Delta N_{\xi} = \sqrt{N_{\xi}}$, and mass $\Delta m_{\xi} = \Delta N_{\xi} v_p (\rho_{particle} - \rho_{fluid})$. In steady state, the buoyancy force acting on these regions, $F_g = \Delta m_{\xi} g$, is equal to the viscous drag force $F_D = 6\pi(1 + \beta_{Re})\eta \xi \Delta V$,

yielding $\Delta V = \Delta m_\xi g / 6\pi(1 + \beta_{Re})\eta\xi$. The term $\beta_{Re} \approx 0.133Re^{0.78}$ is the inertial part of the drag force, valid for $Re \lesssim 30$ [17]. Additionally, because the drag force applies to regions of size ξ , the appropriate Reynolds number is $Re_\xi = 2V\xi/\nu = (\xi/a)Re$. The modified Hinch model then becomes

$$\sigma_V/V \approx 0.6[1 + 0.133([\xi/a]Re)^{0.78}]^{-1}\sqrt{\xi\phi/a}, \quad (2)$$

where the bracketed term represents the influence of particle inertia, and the Hinch model is recovered when $Re \rightarrow 0$ [6]. (We also neglect a prefactor [6], $\gamma(\phi) \equiv \frac{V_0}{V(\phi)} \frac{\eta_0}{\eta(\phi)} \sqrt{S(\phi, 0)} \approx 1.0$ in our semi-dilute samples).

To test this model, we input our fit expression for ξ from Eq. (1) into Eq. (2) and directly compare the predicted values for σ_v/V with our data. As seen in Fig. 3(b), the agreement over the entire range of Reynolds numbers is remarkably good, particularly considering the relative simplicity of the model. The agreement shows that the drop in fluctuation magnitudes with Re is due to both (i) the decreasing correlation lengths ξ and (ii) the increasing drag force term β_{Re} . To illustrate their relative importance, Fig. 3(b) shows the model predictions when the inertial drag force corrections are neglected ($Re = 0$, dashed line). The result shows only a slight decrease with Re , now due solely to the reduction in ξ , and greatly underestimates the observed drop in fluctuation magnitudes. This shows that both terms (i) and (ii) are of similar importance in capturing the behavior of fluctuations at moderate Reynolds numbers.

The value of the Reynolds number, $Re \approx 0.05$, at which inertial effects first appear can be rationalized in two different ways. First, it seems reasonable to expect that when the inertial screening length l becomes similar to the Stokes correlation length ξ_0 , the fluctuations will show an inertial influence. This translates to an onset value $l = a/Re_c \sim \xi_0$, or $Re_c \sim a/\xi_0 \approx 0.04$, in excellent agreement with our estimate of $Re \sim 0.05$ from Fig. 3.

Interestingly, Brenner proposed a different criterion based solely upon a comparison of the particle diffusion coefficient D and the solution viscosity ν [18]. Particle diffusion is driven by velocity fluctuations, and can be estimated from $D = 0.4\xi\sigma_V$ [4, 6, 19]. In the viscous Stokes regime $D \ll \nu$. Brenner argued that if the viscosity is reduced to the point where particle diffusion becomes similar to (viscous) momentum diffusion, $D \sim \nu$, particles will diffuse faster than the momentum they are releasing into the fluid, so that the purely viscous Stokes flow conditions no longer apply. To test this criterion, we plot in Fig. 4 our

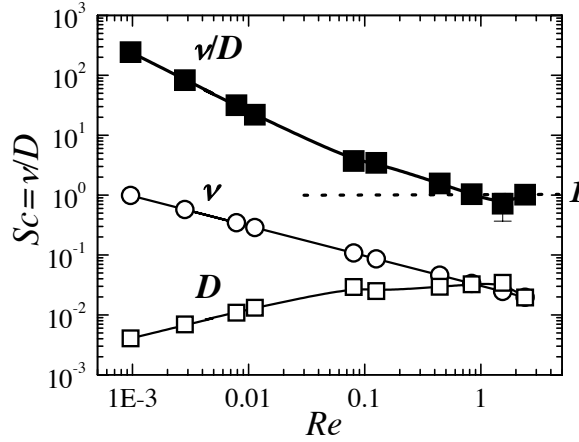


FIG. 4: Fluid kinematic viscosity ν , particle diffusion coefficient $D = 0.4\sigma_V\xi$, and their ratio ν/D (the Schmidt number Sc) vs. Re . The sedimentation dynamics change when D becomes as large as ν . The solid lines are a guide to the eye.

values for ν , D , and the ratio ν/D . The results generally confirm the Brenner picture. The region where $\nu/D \sim 1$ is indeed where significant deviations to Stokes behavior are seen.

Finally, to demonstrate the generality of our results, we re-examine the experiments and conclusions of Cowan *et al.* [14]. They compared many concentrations $0.19 \leq \phi \leq 0.5$, at both $Re_0 = 0.007$ and $Re_0 = 0.3$, and concluded that, contrary to expectations, the velocity fluctuations were independent of Reynolds number for $Re < 1$. We first note that they defined $Re_0 \equiv 2aV_0/\eta_0$ based upon the infinite dilution values V_0 and η_0 , not the values at the high concentrations studied. Using our definition $Re = 2aV/\eta$, we estimate that the $Re_0 = 0.3$ samples range from $0.001 \lesssim Re \lesssim 0.05$. Our critical Reynolds number for the appearance of inertial influence, $Re_c = a/\xi_0$, can also be evaluated from their findings that $\xi \sim 11a\phi^{-1/3}$, resulting in $Re_c \approx 0.06$. We therefore find that $Re \lesssim Re_c$ for *all* of their samples, consistent with their findings of no inertial effects..

The results described here show that the onset of inertial corrections to Stokes sedimentation occurs when the inertial screening length $l = a/Re$ becomes as small as the Stokes velocity correlation length ξ_0 , at Reynolds number $Re_c = a/\xi_0$. At higher Reynolds numbers, inertial screening reduces the size and magnitude of the velocity correlations. The success of the Hinch model in connecting σ_V/V with ξ suggests that the models underlying assumption of a random particle density distribution remains valid in the presence of inertia. These results provide an important benchmark for future theoretical work on moderately

inertial systems.

We thank Tony Ladd for many fruitful discussions.

-
- [1] E. J. Hinch, in *Disorder in Mixing*, edited by E. Guyon et al., Kluwer Academic, Dordrecht, 1988, p. 153.
 - [2] S. Ramaswamy, Adv. in Phys. **50**, 297 (2001).
 - [3] H. Nicolai and E. Guazzelli, Phys. Fluids **7**, 3 (1995).
 - [4] H. Nicolai, B. Herzhaft, E. J. Hinch, L. Oger, and E. Guazzelli, Phys. Fluids **7**, 12 (1995).
 - [5] P.N. Segrè, E. Herbolzheimer and P.M. Chaikin, Phys. Rev. Lett. **79**, 2574 (1997).
 - [6] P.N. Segrè, F. Liu, P. Umbanhower and D.A. Weitz, Nature **409**, 594 (2001).
 - [7] G.B. Michel et al., Phys. Fluids **14**, 2339 (2002).
 - [8] X. Lei, B.J. Ackerson and P. Tong, Phys. Rev. Lett. **86**, 3300 (2001).
 - [9] P.J. Mucha et al., J. Fluid Mech. **501**, 71 (2004).
 - [10] A. Levine, S. Ramaswamy, E. Frey and R. Bruinsma, Phys. Rev. Lett. **81**, 5944 (1998). P. Tong and B.J. Ackerson, Phys. Rev. E **58** (1998). P.J. Mucha and M.P. Brenner, Phys. Fluids **15**, 1305 (2003).
 - [11] G.K. Batchelor, *An Introduction to Fluid Dynamics*, Cambridge University Press, Cambridge, (2002).
 - [12] D.L. Koch and R.J. Hill, Ann. Rev. Fluid Mech. **33**, 619 (2001).
 - [13] D. Koch, Phys. Fluids **5**, 1141 (1993).
 - [14] M.L. Cowan, J.H. Page, and D.A. Weitz, Phys. Rev. Lett. **85**, 453 (2000).
 - [15] R. J. Adrian, Annu. Rev. Fluid Mech. **23**, 261 (1991).
 - [16] R.E. Caflisch and J.H.C. Luke, Phys. Fluids **28**, 259 (1985).
 - [17] B.P. Le Clair et al., J. Atmos. Sci. **27**, 308 (1970).
 - [18] M.P. Brenner, Phys. Fluids **11**, 754 (1999).
 - [19] E. Kuusela and T. Ala-Nissila, Phys. Rev. E **63**, 061505 (2001).